Full paper/Mémoire

Synthesis of colloidal silver nanoparticles for printed electronics

Sarute Ummartyotin [a], Natthaphon Bunnak [a], Julasak Juntaro [b],
Mohini Sain [b],[*], Hathaikarn Manuspiya [a],[*]

[a] The Petroleum and Petrochemical College, Center of Excellence on Petrochemicals and Materials Technology, Chulalongkorn University, 10330 Bangkok, Thailand
[b] Centre for Biocomposites and Biomaterials Processing, Faculty of Forestry, University of Toronto, 33, Willcocks Street, Toronto, M5S 3B3 Canada

A B S T R A C T

Colloidal silver particles were successfully prepared by wet chemical synthesis. The pure single phase of silver was confirmed by X-ray diffraction. Transmission electron microscope categorized that the diameters of particles were 100 and 20 nm, depending on the molecular weight of the PVP stabilizer. A schematic drawing model was used to predict the packing efficiency of 1:1 wt% of two mixtures. The mixture of silver solution was deposited as a thin solid film by a desktop inkjet printer. Scanning electron microscope showed that two different sizes of silver particles give higher densely packed structure than the film of single particle size. When a 0–20 V voltage was applied, the current density reached was 0.10 J/cm^2, suggesting that the silver film has potential to be applied as a cathode layer in organic light emitting diode (OLED) devices.

© 2012 Académie des sciences. Published by Elsevier Masson SAS. All rights reserved.

1. Introduction

Recently, wide attention has been focused on the development of convenience and low-cost processing techniques to deposit conductive features on a nano-bio-composite substrate [1–4] flexible display. Direct-write techniques, one type of printable electronics [5,6] with the feature of low conductive ink consumption, have attracted interest of many industrial applications such as printed circuit board and display device, because they promised the simplification of device manufacturing. Among multiple direct-write technologies, a drop-on demand inkjet printing technology [7–9] is currently used as the high potential method in the printing industry due to low instrument cost and fewer processing steps compared with other patterning processes. In addition, mark-less and non-contact patterning approaches are also beneficial. This technique has been applied to use with a variety of nano-scale materials including ceramics, metal, polymers as well as composites.

Conductive ink solution [10–12], a mixture of metallic particles and organic solution, had been aggitated prior to loading into the inkjet cartridge, in order to prevent agglomeration of particles. The common condition of their particle size must be less than 200 nm and monodispersed. The diameter size of the nozzle of an inkjet cartridge is less than 200 nm, indicated by the printer supplier. In particular, an inkjet printer uses water as media to suspend ink particles. It is desirable that ink particles at the end product should be well aligned and give high electrical conductivity after heat treatment at a relatively low temperature. In the case of metal nanoparticles, when the ink solution was deposited onto the substrate, the solvent was then evaporated with moderate heating and a thin solid film of nanoparticles obtained. The thin solid film was further heated to a higher temperature in order to remove organic molecules and ensure that nanoparticles sinter into a dense metallic film.

In general, nanoparticles are based on monodispersed form. Based on the theoretical maximum density, the attainable packing fraction for the dried film should be 74%

* Corresponding authors.
E-mail addresses: sarute.ummartyotin@utoronto.ca (S. Ummartyotin), m.sain@utoronto.ca (M. Sain), hathaikarn.m@chula.ac.th (H. Manuspiya).

if considering a perfect face-centered cubic lattice. However, the nanoparticle can be randomly packed; this fraction is reduced to 62.5%. Higher dispersions and various different sizes of ink nanoparticles offer larger packing ratio production. In addition, Rasmussen et al. [13] also found that if two different volumes of monodispersed particles were mixed and allowed to be randomly packed, the packing fraction increased and a dense film product can be then obtained.

In this research work, we wish to extend our research work on bio-nanocomposite substrates. Transparent and flexible features of the nanocomposite substrate was successfully investigated. Additional information of the bio-nanocomposite substrate had been discussed elsewhere [3]. The synthesis of silvers nanoparticles for the inkjet printer technique was performed. Silver nanoparticles were prepared as both large and small sizes by the reaction of polyvinylpyrrolidone (PVP) (Mw as 10,000 and 40,000 g/mol), respectively. The silver precursor after the synthetic step was investigated using structural analysis by Fourier transform infrared (FTIR). X-ray diffraction (XRD) and transmission electron microscope (TEM) images were employed to investigate the crystal phase structure and particle size of silver. A schematic drawing model and scanning electron microscope (SEM) images were used to predict and investigate the packing efficiency of the silver thin solid film prepared by desktop inkjet printer. After that, the preliminary experiment of electrical conductivity was performed. This layer was expected to be used as cathode layer in organic light emitting diodes (OLEDs) [14].

2. Materials, instruments and methods

2.1. Materials

AgNO$_3$ (purity > 99.9%) was purchased from Sigma Aldrich Canada and used as the starting material. PVP (10,000 and 40,000 g/mol) was also purchased from Sigma Aldrich Canada and used as stabilizer (purity > 99.9%). Ethylene glycol and methanol were purchased from Bioshop Canada and used as solvent. All of these products were used as received.

2.2. Instruments

2.2.1. Desktop inkjet printer
The Dimatix DMP-2800 inkjet printer (Fujifilm Dimatix, Inc., Santa Clara, CA, USA) was used to deposit the conductive solution on a 50 mm × 50 mm substrate with a disposable piezo inkjet cartridge. The cartridge reservoir contained 2 ml of conductive solution. The temperature of the vacuum plate, which secured the substrate in place, was adjusted to 60 °C.

The conductive solution was prepared as 1:1 by weight of a mixture of the two precursor sources from the synthetis step and adding 10 wt% of deionized water. Conductive solution was filtered by nano-size filter (200 nm) before usage in order to prevent agglomeration among silver particles.

2.2.2. Attenuated total reflectance Fourier transform infrared (ATR-FTIR)
ATR-FTIR was performed on a Bruker Vector 22 mid-IR spectroscopy (Bruker, Germany), equipped with an ATR crystal (50 mm × 10 mm × 2 mm) at 45° incident angle configuration. All FTIR absorption spectra were recorded over 4500–500 cm^{-1} wavenumbers region at a resolution of 8 cm^{-1} with 1024 scans using a deuterated triglycine sulfate (DTGS) detector. A straight line between two lowest points in the respective spectra region was chosen as a baseline, and the peak areas were integrated from 2000–500 cm^{-1}. The position peak of C–H and C–O stretching region will be compared with literature [15].

2.2.3. Transmission electron microscope (TEM)
The particle size of silver was investigated by TEM, using a Hitachi H-7000. The silver solution was suspended in methanol and dropped on a molybdenum grid. After that, the grid was dried at 50 °C for methanol evaporation and kept into the TEM chamber. The obtained image was computer processed for identification of the domains in which certain lattice fringes appear. For this propose, TEM image was captured under 60 k × and 150 k × magnification. The acceleration voltage of electron beam was set at 100 keV.

2.2.4. X-ray diffraction (XRD)
After silver particles were printed on the substrate, the process of heat treatment was conducted for solvent removal; a thin solid film of silver can be then obtained. The crystal structure of the silver film was identified by XRD (Phillips P.W. 1830 diffractometer) using nickel-filtered CuKα radiation. Diffraction patterns were recorded over a range of 2θ angles from 25–80°. The consistent results were compared with literature [15].

2.2.5. Scanning electron microscope (SEM)
The thin solid film of silver was investigated by SEM (a JOEL JSM-6301F scanning microscope). The machine was operated at an acceleration voltage of 20 keV; a working distance of 15 mm and a magnification of 30 k × were used to identify the dense characteristic of thin solid film of silver.

2.2.6. I-V probe station
The thin solid film of silver was investigated for the relationship of current density and applied voltage by I-V probe station. The forward bias was applied in the range of 0–20 V. The range of applied voltage for OLEDs was suggested by literature [4,14].

2.3. Methods

2.3.1. Synthesis of silver nanoparticle and characterization
Colloidal silver particles were synthesized by polyol process. The large particle size of silver colloid was synthesized by dissolving 1 g of 10,000 molecular weight PVP in 4 ml of ethylene glycol. Then, the solution was heated to 130 °C and left until PVP has dissolved. In parallel, 1 g of AgNO$_3$ was also dissolved in 4 ml of ethylene glycol and heated to 130 °C. PVP solution was then poured

into AgNO$_3$ solution. The combined solution was maintained at 130 °C for 4 h before cooled down to room temperature. Once the colloid was synthesized, 10 ml of methanol was added and then the colloid was centrifuged at 500 rpm for 30 min. The solvent was removed and colloid was kept in oven at 150 °C.

For the small particle size of colloid, the synthesis followed the similar procedure as the large particle size preparation. The 40,000 molecular weight of PVP was used instead of the 10,000 molecular weight.

To mix silver particles of the two different sizes, both post-reaction of silver precursors were mixed and stirred at room temperature for 2 h to obtain a homogeneous product of silver precursor mixture.

Then, the silver precursor was characterized by FTIR for chemical structure analysis. Solid particles after the centrifugation step were then investigated by means of TEM and XRD for particle size and crystal phase structure, respectively.

2.3.2. Silver nanoparticle thin film preparation and characterization

The solutions of large and small of silver particle sizes as well as the mixture of both were dissolved in 3 ml of water and loaded into the cartridge reservoir of the desktop inkjet printer. Each of three ink formulations was sonicated for 3 h prior to printing in order to prevent the agglomeration among ink particles. Then, the amount of solution and plate temperature was controlled at 3 ml at 50 °C. After that, the deposited silver film was dried at 180 °C over night.

The silver thin films were characterized by SEM for morphological analysis of the surface. Then, the preliminary experiment of electrical conductivity measurement was conducted by I-V probe station.

3. Results and discussion

3.1. Dissociation of silver nitrate

In this experiment, silver nanoparticles were successfully synthesized by use of polymer in wet chemical synthetic route. PVP was used as the stabilizer for nanoscale size-of-particle control. The embedding of such particles in the PVP matrix is also advantageous. The formation of silver particles was synthesized from silver ions using a reducing agent. It can be trapped along the PVP
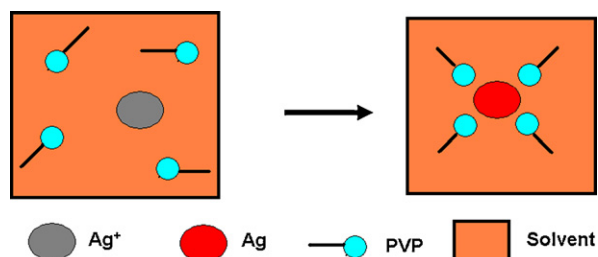
chain and the size of this particle can be controlled into nanoscale. It can be explained that PVP can prevent the agglomeration and precipitation among each particle size. The bulk particle of silver can be avoided.

On the other hand, in common theory, it is remarkable to note that silver nitrate has the highest lattice energy when comparing to any other silver salt and therefore, it can be dissolved only in polar solvents. The silver ion is a powerful oxidant and can be reduced to metal silver, which can be proved by the similar result in the previous report [16]. In our case, silver nitrate was dissolved in ethylene glycol in order to synthesize silver nanoparticles in the organic phase. The chemical reaction requires that some of the organic molecules can dissociate lattices of silver nitrate and form organic-soluble complexes as shown in Fig. 1. PVP, one type of organic molecule, was used to dissociate silver ions. PVP acts as a protective agent and restricts the mobility of silver ions during the reaction, controlling most of the agglomeration. The in situ produced silver ions were bound to PVP through a chemical bonding which later helps silver ions to get converted into silver. According to related theory, it can be explained that the coordinative interaction between organic molecule and metal is related to electron donation from the organic molecule to the metal atom and electron reverse-donation from the metal atom to the organic molecule [17].

FTIR spectroscopy was used to investigate the neat PVP solution, thin solid films of silver and coordinative interaction between silver ions and PVP solution.

Fig. 2 exhibits FTIR spectra of pure silver, PVP solution and mixture of silver nanoparticles dispersed in PVP solution. For the PVP solution, it can be found that the pattern of PVP molecules exhibited absorption peaks at wavenumbers of 1663 and 1180 cm^{-1}. These corresponded to C=C stretching and saturated C–O vibration, respectively. In addition, it can be observed that the intensity pattern of the mixture of pure silver nanoparticles and PVP solution was slightly decreased from pure PVP solution. It can be explained that neat silver nanoparticles, generally exhibited as neat colloidal nanoparticles, may disturb the adsorption on PVP molecule. On the other hand, for the

Fig. 1. Illustration of direct chemical synthetic route of silver nanoparticle from the reaction of silver nitrate and polyvinylpyrrolidone (PVP) solution.
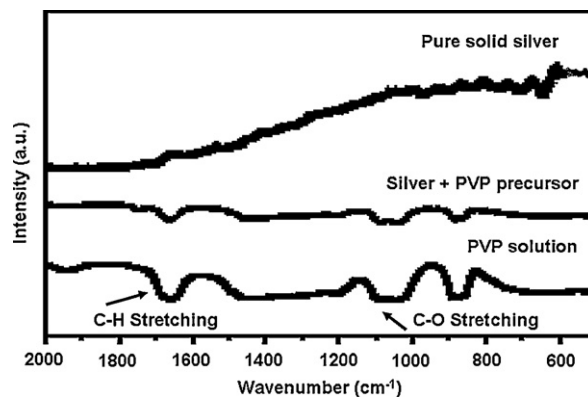
Fig. 2. Fourier transform infrared (FTIR) spectra of pure silver, polyvinylpyrrolidone (PVP) solution, mixture of pure silver nanoparticle and PVP solution.
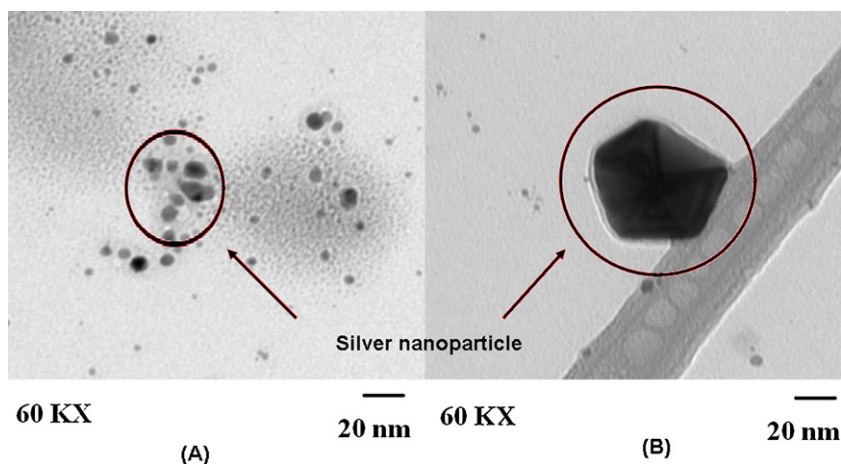
Fig. 3. Transmission electron microscope of silver nanoparticle. A. Silver nanoparticle prepared from polyvinylpyrrolidone (PVP) (Mw~40,000). B. Silver nanoparticle prepared from PVP (Mw~10,000) at 60 k × magnifications.
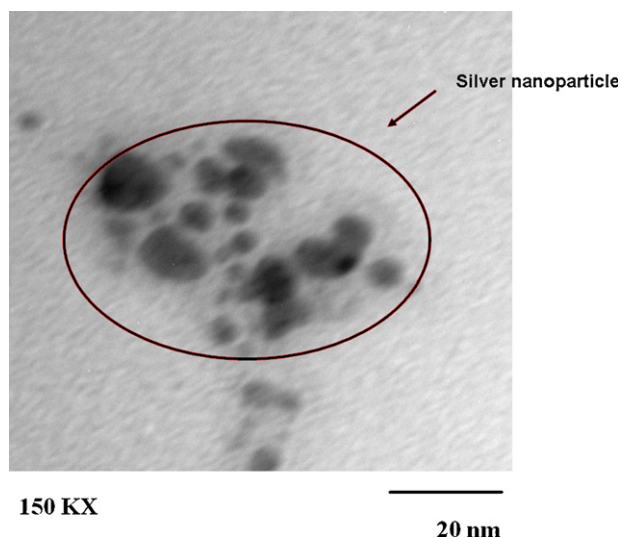
Fig. 4. Transmission electron microscope of silver nanoparticle prepared from polyvinylpyrrolidone (PVP) (Mw~40,000) at 150 k × magnification.

silver film, the spectra exhibited a featureless character over the identical wavenumbers. It can be interpreted that the organic molecule from PVP solution was completely removed after centrifugation and annealing at 200 °C. There is only silver nanoparticles. This result was consistent with the XRD result.

3.2. Silver nanoparticle formation

The particle size, microstructure and size distribution of synthetic nanoparticles were characterized via TEM. Fig. 3 indicates that a homogeneous distribution of the nanoparticles can be observed. The smaller size of nanoparticles was prepared in PVP (Mw ~40,000) with a diameter of roughly 20 nm, while the larger ones were prepared in PVP (Mw ~10,000) with a diameter of roughly 100 nm. The results were consistent with XRD observation. The size
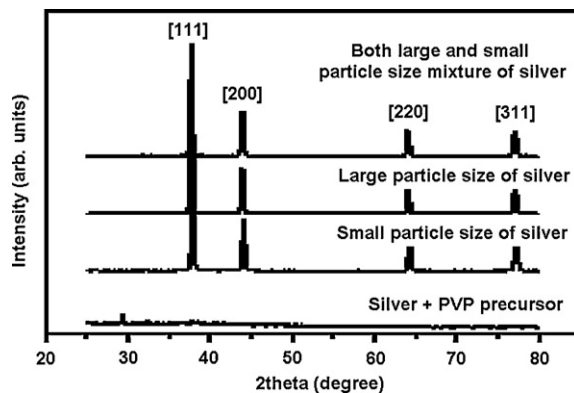
Fig. 5. X-ray diffraction of silver nanoparticle.
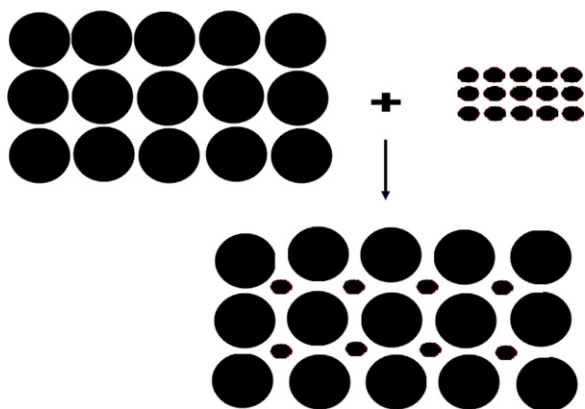
Fig. 6. Schematic drawing of ideal arrangement of small and large particles in printed silver lines.

distribution of both small and large silver nanoparticles was quite uniform. In particular, a very large size and non-spherical shape particle can be seen at higher magnification in Fig. 4. It is important to note that the PVP solution plays an important role in stabilizing the suspension of silver particles and prevents them from agglomerating.

XRD was used to investigate the crystalline structure of the materials. Fig. 5 exhibits the XRD patterns of specimens deposited with different silver particle sizes. No silver diffraction peak was detected for the mixture of silver nitrate and PVP solution. The precursor solution did not contain the crystallite structure of silver. More diffraction peaks appeared in the case of silver thin film deposition including large, small of silver particle size and the mixture of these. The peaks can be remarkably observed at 37.5°,

43.7°, 63.9° and 76.8° corresponding to the face-centered cubic structure of silver crystal planes (111), (200), (220) and (311) of silver metal which are consistent with those of bulk silver [18,19]. It can be determined that silver is well crystallized. In Fig. 5, it is evident that the intensity of the diffraction peak increased from the small particle size to large particle size and the mixture of these due to higher density thin film materials. This is consistent with the previous report [20,21]. In addition, the particle sizes of silver nanocrystals can be calculated from the peaks of XRD spectra based on the Scherrer's equation:

$$D = k\lambda/(\beta\cos\theta)$$

where D is the distance between plan which is proportional to the average particle size, k is a constant taken as 0.9 for calculation, β is the full width at half maximum (FWHM) in radians, λ is the wavelength of the X-ray, and θ is the diffraction angle. From the Scherrer's equation, the particle size of synthesized silver has been calculated to be roughly 26 nm and 110 nm for the expected small and large particle size based on the (111) peak, respectively. This is close to the value deduced from TEM images.

3.3. Silver thin film preparation, packing efficiency of silver nanoparticles and electrical conductivity

Both large and small sizes of silver nanoparticles were successfully synthesized from wet chemical synthetic route. The mixture of both large and small particle sizes was performed in order to enhance the electrical properties and to prevent crack [22] and pinhole [23] phenomena, while thin solid film of silver was fabricated as the electrode layer of an electronic device. The crack and
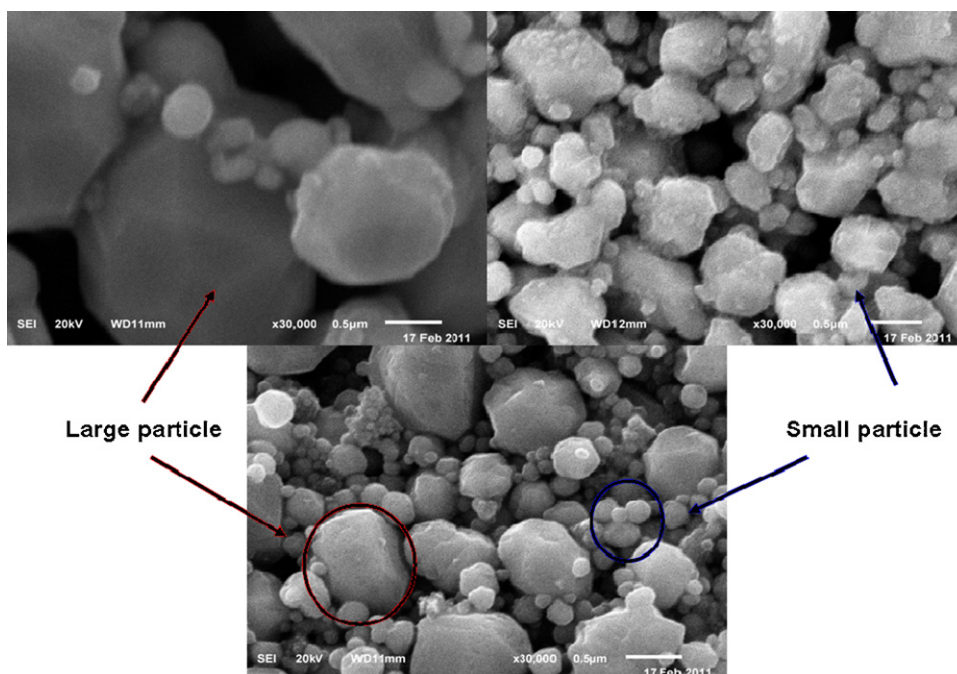
Fig. 7. Scanning electron microscope (SEM) image of silver nanoparticle at 30 k × magnification.
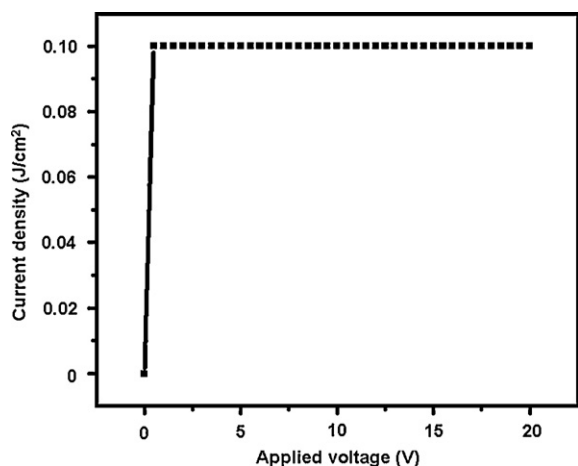
Fig. 8. Current density (J/cm^2) versus applied voltage (V) for synthesis of silver thin film.

pinhole phenomena can occur at the grain boundary of the silver film or free spaces among silver particles. The connection between grains of silver is easily to crack due to higher residual stress when silver film is bent. The free space among silver particles exhibits less amount of silver, so when silver film is bent, the non-connection between aligned silver occurred.

Fig. 6 represents the schematic drawing model. It was used to predict the two dimensional packing of silver nanoparticles. In order to prevent the occurrence of space among large particles of silver colloid, smaller particles can fill in this space. The combination of both large and small particle sizes of silver colloid was expected to provide a dense thin solid film of silver.

After the heating step, both large and small particle sizes of silver were well packed. The free space among silver particles in the mixture case is less than the individual ones. In Fig. 7, the dried silver of both large and small particle sizes provided the average diameter as 100 and 20 nm, respectively. However, each procedure of both synthetic steps may offer a significant amount of polydispersity in particle size. The size of silver particles may be higher or lower of 100 and 20 nm. After silver particles were heated to 200 °C for solvent evaporation, the free space can be then observed. In case of small particle size (right top), the large space was not well observed, while this is opposite for large particle size (left top). In case of the large and small particle size mixture, the dried silver film exhibited denser packing than film of only large or small particle size. The necking area among particles was expected to enhance when silver dried film was heated with higher temperature [24,25].

Once silver nanoparticles were printed as a thin solid film, the relationship of current density and applied voltage was measured using I-V probe station. From the measurement in Fig. 8, under forward bias voltage from

0–20 V, the current density exhibited as 0.1 J/cm^2. This constant current density and range of applied voltage are commonly utilized for OLEDs device [4,14]. All the measurements were conducted at ambient atmosphere with no encapsulation. The consistent result of our synthesized silver offered the identical data as the commercial silver paint electrode. The preliminary experiment of electrical conductivity was successfully performed for further development of cathode layer in OLEDs in the near future.

4. Conclusion

Dense thin solid films of silver were successfully developed. From the ease of synthetic route, both large (100 nm) and small (20 nm) particle sizes of silver were successfully synthesized. The mixture of both large and small particle sizes of silver solution was printed as a thin solid film of silver. The preliminary experiment of electrical conductivity suggested that it can be applied as the cathode layer for OLEDs device.

Acknowledgement

References

[1] M. Nogi, H. Yano, Adv. Mater. 20 (2008) 1849.
[2] Y. Okahisa, et al. Composites Sci. Technol. 69 (2009) 1958.
[3] C. Wu, Production and characterization of optically transparent nano-composite film in Faculty of Forestry, University of Toronto, Toronto, 2010.
[4] C. Legnani, et al. Thin Solid Films 517 (2008) 1016.
[5] T.I. Sultan, Comput. Ind. 7 (1986) 537.
[6] J. Vlietstra, Comput. Ind. 1 (1979) 41.
[7] S. Jeong, et al. J. Appl. Phys. 102805 (2010) 1.
[8] I. Kim, J. Kim, J. Appl. Phys. 102807 (2010) 1–5.
[9] B.J. Park, et al. J. Appl. Phys. 102803 (2010) 1.
[10] C.N. Chen, et al. Appl. Surf. Sci. 257 (2010) 650.
[11] A. Gloskovskii, et al. Thin Solid Films 518 (2010) 4030.
[12] A. Michna, et al. J. Colloid Interface Sci. 345 (2010) 187.
[13] S.T. Rasmussen, et al. Dent. Mater. 13 (1997) 43.
[14] B. Geffroy, P. Le Roy, C. Prat, Polym. Int. 55 (2006) 572.
[15] K.J. Lee, et al. J. Colloid Interface Sci. 304 (2006) 92.
[16] X. Sun, S. Dong, E. Wang, J. Colloid Interface Sci. 288 (2005) 301.
[17] A.N. Widmer-Copper, L.F. Lindoy, J.R. Reimers, J. Phys. Chem. A 105 (2001) 6567.
[18] W. Song, et al. J. Colloid Interface Sci. 298 (2006) 765.
[19] H. Qi, et al., Controlled assembly of gold and silver nanoparticles using thermotropic amphiphilic and conventional liquid crystals, in: 5th IEEE conference on nanotechnology, Nagoya, Japan, 2005.
[20] S.P. Ramnani, et al. Catalyst Commun. 9 (2008) 756.
[21] W. Yan, et al. J. Mol. Catalyst A Chem. 225 (2006) 81.
[22] S. Olliges, et al. Scripta Materialia 58 (2008) 175.
[23] G. Mouret, et al. J. Aerosol Sci. 40 (2009) 762.
[24] K.C. Yung, et al. J. Mater. Proc. Technol. 210 (2010) 2268.
[25] J.C. Lin, W. Wu, Mater. Chem. Phys. 40 (1995) 110.